Coupled Systems Mechanics, *Vol. 11, No. 5 (2022) 389-409*
https://doi.org/10.12989/csm.2022.11.5.389

Dynamic of behavior for imperfect FGM plates resting on elastic foundation containing various distribution rates of porosity: Analysis and modeling

Aicha Kablia[1,2], Rabia Benferhat[1,2] and Hassaine Daouadji Tahar*[1,2]

[1]*Department of Civil Engineering, University of Tiaret, Algeria*
[2]*Laboratory of Geomatics and Sustainable Development, University of Tiaret, Algeria*

(Received July 5, 2021, Revised May 16, 2022, Accepted May 24, 2022)

Abstract. During the manufacture of FGM plates, defects such as porosities can appear. Those can change the entire behavior of these plates. This paper aims to investigate the free vibration characteristics of porous functionally graded (FG) plates resting on elastic foundations. The Young's modulus of the plate is assumed to vary continuously through the thickness according to a power-law formulation, and the Poisson ratio is held constant. Different types of porosity distribution rates are considered. To examine the accuracy of the present formulation, several comparison studies are investigated. Effects of variation of porosity distribution rate, foundation parameter, power-law index and thickness ratio on the fundamental frequency of plates have been investigated.

Keywords: elastic foundation; free vibration analysis; functionally graded plate; imperfect plates; porosity distribution rate

1. Introduction

Functionally graded materials (FGMs) are a class of composites that have a continuous variation of material properties from one surface to another and thus eliminate the stress concentration found in laminated composites. The concepts of FGMs were proposed by material scientists in the Sendai area of Japan. Typically, FGM is made from a mixture of ceramic and metal in such a way that the ceramic can resist high temperatures in thermal environments, whereas the metal can decrease the tensile stress occurring on the ceramic surface at the earlier state of cooling. Material properties such as elasticity modulus, shear modulus, mass density, and Poisson's ratio are varying smoothly and continuously from one surface to another in the desired direction. It is difficult to obtain an exact enough solution to the nonlinear equations to develop efficient mathematical models to predict the static and dynamic response of a plate. Thus far, only a few exact solutions have been investigated. However, with progress in science and technology, a need arises in engineering practice to accurately predict the nonlinear static and dynamic responses of a plate (Keleshteri *et al*. 2017, Bekki *et al*. 2019, Keleshteri *et al*. 2017b, Kamran *et al*. 2020,

*Corresponding author, Professor, E-mail: daouadjitahar@gmail.com

http://www.techno-press.org/?journal=csm&subpage=8 ISSN: 2234-2184 (Print), 2234-2192 (Online)

Adim *et al*. 2016b, Belkacem *et al*. 2016b, Bourada 2020, Benhenni *et al*. 2019, Kablia *et al*. 2020, Tlidji *et al*. 2021a, Chaabane *et al*. 2019, Abdelhak *et al*. 2021, Adim *et al*. 2018, Chikr *et al*. 2020, Anqiang *et al*. 2020, Belkacem *et al*. 2016a, Keleshteri *et al*. 2022, Hua *et al*. 2020, Reza *et al*. 2020).

Plates supported by elastic foundations have been widely adopted by many researchers to model various engineering problems during the past decades. To describe the interactions of the plate and its foundation as appropriately as possible, scientists have proposed various kinds of foundation models (Kerr 1964). The simplest model for the elastic foundation is the Winkler model, which regards the foundation as a series of separated springs without coupling effects between each other, resulting in the disadvantage of discontinuous deflection on the interacted surface of the plate. This was later improved by Pasternak, who exploited the interactions between the separated springs in the Winkler model by introducing a new dependent parameter. From then on, the Pasternak model was widely used to describe the mechanical behavior of the structure-foundation interactions (Xiang *et al* 1994, Abdelhak *et al*. 2016, Adim *et al*. 2016a, Benferhat *et al*. 2021, Benferhat *et al*. 2016a, Benferhat *et al*. 2016b, Benferhat *et al*. 2019, Benferhat *et al*. 2020, Bekki *et al*. 2021, Benhenni *et al*. 2018, Tlidji *et al*. 2021b, Zhou *et al.* 2004). Nowadays, there has been a great research effort to analyze static, buckling and vibration of FGM structures. Keleshteri *et al*. (2019) used the third-order shear deformation theory (TSDT) in conjunction with the nonlinear von Karman strain field to analyzed the nonlinear bending behavior of functionally graded carbon nanotube reinforced composite (FG-CNTRC) annular plates with variable thickness on an elastic foundation. Ta and Noh (2015) presented a new refined plate theory for dynamic analysis of functionally graded (FG) plate resting on the Pasternak foundation under the transverse loading. In a paper by Thai and Kim (2013), buckling analysis of thick FG plate resting on elastic foundation was examined and some closed-form solutions are presented. Keleshteri *et al*. (2018) analyzed postbuckling behavior of FG-CNTRC rectangular plates with integrated piezoelectric layers subjected to different in-plane compressive loads.Taczała *et al*.(2015) investigated the stability of thermally loaded FG plates resting on an elastic foundation with the help of finite element method. Anqiang *et al*. (2020) Investigated the effect of porosity distributions on vibrational behavior of FG sectorial plates resting on a two-parameter elastic foundation. In a paper by Huang *et al*. (2012), free vibration of rectangular FG plates with through internal cracks is studied by means of Ritz method and the three-dimensional elasticity theory. Li and Zhang (2016) investigated free vibration of a rotating cantilever FG plate undergoing large overall motions using a dynamic model with the dynamic stiffening effect. Keleshteri *et al*. (2017a) established nonlinear dynamic equations using first-order shear deformation theory in conjunction with von Karman geometrical nonlinearity large amplitude vibration analysis of FG-CNTRC annular sector plates with surface bonded piezoelectric layers. Lal and Ahlawat (2015) presented some important results for the axisymmetric vibrations of FG plates under uniform in-plane force using the differential transform method based on classical plate theory. Hassaine Daouadji *et al*. (2016) suggested a new displacement model to analyze the static behavior of FG plates. Belabed *et al*. (2014) improved a new higher order shear and normal deformation theory for bending and free vibration analyses of FG plates. Hongwei *et al*. (2020) investigated free vibration of FG sandwich annular sector plates on Pasternak elastic foundation with different boundary conditions, based on the three-dimensional theory of elasticity. Ramu and Mohanty (2014) improved a finite element formulation for modal analysis of FG plates based on the Kirchhoff plate theory. Shariati *et al*. (2020) investigated the vibration characteristics of flexoelectric nanobeams resting on viscoelastic foundation and subjected to magneto-electro-viscoelastic-hygro-thermal (MEVHT) loading.

Mohammadimehr *et al*. (2020) studied the buckling analysis of sandwich composite (carbon nanotube reinforced composite and fiber reinforced composite) Euler-Bernoulli beam in two configurations using differential quadrature method (DQM). The large amplitude vibration of FG plates under random pressure in thermal environment with finite element modal reduction method was studied by Parandvar and Farid (2015). Keleshteri *et al*. (2020) utilized the von Karman geometrical nonlinearity along with the Hamilton principle to study the large amplitude free vibration response of functionally graded porous (FGP) cylindrical panels considering different shell theories and boundary conditions. Sator *et al*. (2016) studied transient vibration analysis problems for FG plates under transversal dynamic loading using three different plate theories. Talha *et al*. (2010) established free vibration and static analysis of functionally graded material (FGM) plates using higher-order shear deformation theory with a special modification in the transverse displacement in conjunction with finite element models. Tran *et al*. (2015) suggested a novel and effective formulation based on combining the extended isogeometric approach and the higher-order shear deformation theory for dynamic analysis of the cracked FG plates. Parveen *et al*. (2021) studied the deformation in a homogeneous isotropic thermoelastic solid using modified couple stress theory subjected to inclined load with two temperatures with multi-dual-phase-lag heat transfer. Fenjan *et al*. (2020) used the differential quadrature (DQ) method to study the free vibrations of porous functionally graded (FG) micro/nano beams in thermal environments. Zhang and Zhou (2015) proposed a model for FG plates lying on nonlinear elastic foundations by means of the concept of physical neutral surface and high-order shear deformation theory. In a paper by Parandvar and Farid (2016), dynamic response of FG plates subjected simultaneously to thermal, static, and harmonic loads was investigated by means of nonlinear finite element method. In Thai *et al*. (2016) presented a new simple four-unknown shear and normal deformation theory for static, dynamic and buckling analyses of FG plates.

The novelty of this work is to study the effect of the variation of the porosity distribution rate on the dynamic behavior of FGM plates by the use of new mixture laws. Numerical examples are presented to illustrate the precision and the efficiency of the present solution, by showing the influence of the distribution rate of the porosity of the base material on the mechanical behavior of the FGM plate.

2. Problem formulation

2.1 Constitutive relations of (metal/ceramic) FGM plates

Consider an imperfect FGM with a porosity volume fraction, α ($\alpha << 1$), distributed evenly among the metal and ceramic, the modified rule of mixture proposed by Wattanasakulpong and Ungbhakorn (2014) is used as (Benferhat *et al*. 2016)

$$P = P_m(V_m - \frac{\alpha}{2}) + P_c(V_c - \frac{\alpha}{2}) \tag{1}$$

Now, the total volume fraction of the metal and ceramic is: V_m+V_c=1 and the power law of volume fraction of the ceramic is described as (Table 1)

$$V_c = (\frac{z}{h} + \frac{1}{2})^k \tag{2}$$

Table 1 Summary table which groups the different distribution of porosity in the FGM (Ceramic/Metal)

Distribution of porosity rate in the FGM			Young module	
Type	Ceramic	*Metal*		
Type-I	Without porosity		$E(z) = (E_c - E_m)(\frac{z}{h} + \frac{1}{2})^k + E_m$(Wattanasakulponga 2014)	(19)
Type-II	50%	50%	$E(z) = (E_c - E_m)(\frac{z}{h} + \frac{1}{2})^k + E_m - (E_c + E_m)\frac{\alpha}{2}$	(20)
Type-III	60%	40%	$E(z) = (E_c - E_m)(\frac{z}{h} + \frac{1}{2})^k + E_m - (3E_c + 2E_m)\frac{\alpha}{5}$	(21)
Type-IV	40%	60%	$E(z) = (E_c - E_m)(\frac{z}{h} + \frac{1}{2})^k + E_m - (2E_c + 3E_m)\frac{\alpha}{5}$	(22)
Type-V	75%	25%	$E(z) = (E_c - E_m)(\frac{z}{h} + \frac{1}{2})^k + E_m - (3E_c + E_m)\frac{\alpha}{4}$	(23)
Type-VI	25%	75%	$E(z) = (E_c - E_m)(\frac{z}{h} + \frac{1}{2})^k + E_m - (E_c + 3E_m)\frac{\alpha}{4}$	(24)

Hence, all properties of the imperfect FGM can be written as (Benferhat *et al*. 2016a)

$$\rho(z) = (\rho_c - \rho_m)(\frac{z}{h} + \frac{1}{2})^k + \rho_m - (\rho_c + \rho_m)\frac{\alpha}{2} \tag{3}$$

It is noted that the positive real number k ($0 \leq k < \infty$) is the power-law or a volume fraction index, and z is the distance from the mid-plane of the FG plate. The FG plate becomes a fully ceramic plate when k is set to zero and fully metal for large value of k.

Thus, the equations of Young's modulus (E) and material density (ρ) of the imperfect MGF plate can be expressed as (Benferhat *et al*. 2016a), including a summary table which groups together the different porosity distributions in the FGMs will be presented in Table 1.

$$E(z) = (E_c - E_m)(\frac{z}{h} + \frac{1}{2})^k + E_m - (E_c + E_m)\frac{\alpha}{2} \tag{4}$$

$$\rho(z) = (\rho_c - \rho_m)(\frac{z}{h} + \frac{1}{2})^k + \rho_m - (\rho_c + \rho_m)\frac{\alpha}{2} \tag{5}$$

However, Poisson's ratio (ν) is assumed to be constant. The material properties of a perfect FG plate can be obtained when α is set to zero.

$$\text{As: } V_c + V_m = 1 \Rightarrow V_c = 1 - V_m \tag{6}$$

$$\text{and: } V_c = (\frac{z}{h} + \frac{1}{2})^k \tag{7}$$

Type I: *perfect FG plate (Without porosity $\alpha = 0$)*

$$E(z) = (E_c - E_m)(\frac{z}{h} + \frac{1}{2})^k + E_m \tag{8}$$

Type II: *50% Ceramic, 50% Metal*

$$E = E_m(V_m - \frac{\alpha}{2}) + E_c(V_c - \frac{\alpha}{2}) \tag{9}$$

$$E(z) = (E_c - E_m)(\frac{z}{h} + \frac{1}{2})^k + E_m - (E_c + E_m)\frac{\alpha}{2} \tag{10}$$

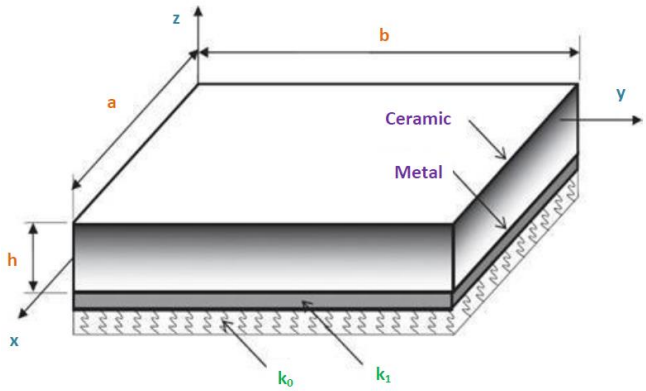

Fig. 1 Geometry and dimensions of the FGM plate resting on elastic foundation

Type III: *60% Ceramic, 40% Metal*

$$E = E_m(V_m - \frac{2\alpha}{5}) + E_c(V_c - \frac{3\alpha}{5}) \tag{11}$$

$$E(z) = (E_c - E_m)(\frac{z}{h} + \frac{1}{2})^k + E_m - (3E_c - 2E_m)\frac{\alpha}{5} \tag{12}$$

Type IV: *40% Ceramic, 60% Metal*

$$E = E_m(V_m - \frac{3\alpha}{5}) + E_c(V_c - \frac{2\alpha}{5}) \tag{13}$$

$$E(z) = (E_c - E_m)(\frac{z}{h} + \frac{1}{2})^k + E_m - (2E_c - 3E_m)\frac{\alpha}{5} \tag{14}$$

Type V: *75% Ceramic, 25% Metal*

$$E = E_m(V_m - \frac{\alpha}{4}) + E_c(V_c - \frac{3\alpha}{4}) \tag{15}$$

$$E(z) = (E_c - E_m)(\frac{z}{h} + \frac{1}{2})^k + E_m - (3E_c - E_m)\frac{\alpha}{4} \tag{16}$$

Type VI: *25% Ceramic, 75% Metal*

$$E = E_m(V_m - \frac{3\alpha}{4}) + E_c(V_c - \frac{\alpha}{4}) \tag{17}$$

$$E(z) = (E_c - E_m)(\frac{z}{h} + \frac{1}{2})^k + E_m - (E_c - 3E_m)\frac{\alpha}{4} \tag{18}$$

2.2 Displacement fields and strains

In this study, we consider an FGM plate of length a, width b and total thickness h and composed of functionally graded material through the thickness. It is assumed that the material is isotropic and grading is assumed to be only through the thickness. The xy plane is taken to be the undeformed mid plane of the plate with the z axis positive upward from the mid plane. The material on the top surface and bottom surface is ceramic and metal respectively (Fig. 1).

The assumed displacement field is as follows (Baferani *et al*. 2011, Ait Atmane. 2019, Tounsi *et al*. 2020)

$$\begin{gathered} u(x,y,z) = u_0(x,y) - z\frac{\partial w_b}{\partial x} - (z - \sin(\frac{\pi z}{h}))\frac{\partial w_s}{\partial x} \\ v(x,y,z) = v_0(x,y) - z\frac{\partial w_b}{\partial y} - (z - \sin(\frac{\pi z}{h}))\frac{\partial w_s}{\partial y} \\ w(x,y,z) = w_b(x,y) + w_s(x,y) \end{gathered} \tag{25}$$

where u_0 and v_0 are the mid-plane displacements of the plate in the x and y direction, respectively; w_b and w_s are the bending and shear components of transverse displacement, respectively, while $f(z)$ represents shape functions determining the distribution of the transverse shear strains and stresses along the thickness and is given as (Benferhat *et al*. 2016a)

$$f(z) = z - \sin(\frac{\pi z}{h}) \tag{26}$$

It should be noted that unlike the first-order shear deformation theory, this theory does not require shear correction factors. The kinematic relations can be obtained as follows

$$\begin{gathered} \varepsilon_x = \varepsilon_x^0 + z\,k_x^b + (z - \sin(\frac{\pi z}{h}))\,k_x^s \\ \varepsilon_y = \varepsilon_y^0 + z\,k_y^b + (z - \sin(\frac{\pi z}{h}))\,k_y^s \\ \gamma_{xy} = \gamma_{xy}^0 + z\,k_{xy}^b + (z - \sin(\frac{\pi z}{h}))\,k_{xy}^s \\ \gamma_{yz} = (1 - \frac{d(z-\sin(\frac{\pi z}{h}))}{dz})\,\gamma_{yz}^s \\ \gamma_{xz} = (1 - \frac{d(z-\sin(\frac{\pi z}{h}))}{dz})\,\gamma_{xz}^s \\ \varepsilon_z = 0 \end{gathered} \tag{27}$$

where

$$\varepsilon_x^0 = \frac{\partial u_0}{\partial x},\ k_x^b = -\frac{\partial^2 w_b}{\partial x^2},\ k_x^s = -\frac{\partial^2 w_s}{\partial x^2}, \gamma_{xy}^0 = \frac{\partial u_0}{\partial y} + \frac{\partial v_0}{\partial x}, k_{xy}^s = -2\frac{\partial^2 w_s}{\partial x \partial y}$$

$$\varepsilon_y^0 = \frac{\partial v_0}{\partial y},\ k_y^b = -\frac{\partial^2 w_b}{\partial y^2},\ k_y^s = -\frac{\partial^2 w_s}{\partial y^2}, k_{xy}^b = -2\frac{\partial^2 w_b}{\partial x \partial y}, \gamma_{xz}^s = \frac{\partial w_s}{\partial x} \tag{28}$$

$$\gamma_{yz}^s = \frac{\partial w_s}{\partial y},\ g(z) = 1 - f'(z) = 1 - \frac{d(z-sin(\frac{\pi z}{h}))}{dz}, f'(z) = \frac{d(z-sin(\frac{\pi z}{h}))}{dz}$$

The stress state in each layer is given by Hooke's law

$$\begin{Bmatrix} \sigma_x \\ \sigma_y \\ \tau_{yz} \\ \tau_{xz} \\ \tau_{xy} \end{Bmatrix} = \begin{bmatrix} \frac{E(z)}{1-\nu^2} & \frac{\nu E(z)}{1-\nu^2} & 0 & 0 & 0 \\ \frac{\nu E(z)}{1-\nu^2} & \frac{E(z)}{1-\nu^2} & 0 & 0 & 0 \\ 0 & 0 & \frac{E(z)}{2(1+\nu)} & 0 & 0 \\ 0 & 0 & 0 & \frac{E(z)}{2(1+\nu)} & 0 \\ 0 & 0 & 0 & 0 & \frac{E(z)}{2(1+\nu)} \end{bmatrix} \begin{Bmatrix} \varepsilon_x \\ \varepsilon_y \\ \gamma_{yz} \\ \gamma_{xz} \\ \gamma_{xy} \end{Bmatrix} \tag{29}$$

2.3 Governing equations

The governing equations of equilibrium can be derived by using the principle of virtual displacements. The principle of virtual work in the present case yields (Baferani *et al*. 2011, Ait Atmane. 2019, Tounsi *et al*. 2020)

$$\int_{-h/2}^{h/2}\int_{\Omega}\left[\sigma_x\delta\,\varepsilon_x+\sigma_y\delta\,\varepsilon_y+\tau_{xy}\delta\,\gamma_{xy}+\tau_{yz}\delta\,\gamma_{yz}+\tau_{xz}\delta\,\gamma_{xz}\right]\,d\Omega\,dz-\int_{\Omega}q\,\delta\,w d\Omega=0 \tag{30}$$

where Ω is the top surface and q is the applied transverse load.

Substituting Eqs. (27) and (29) into Eq. (30) and integrating through the thickness of the plate, Eq (30) can be rewritten as

$$\begin{aligned}&\int_{\Omega}\left[N_x\delta\,\varepsilon_x^0+N_y\delta\,\varepsilon_y^0+N_{xy}\delta\,\varepsilon_{xy}^0+M_x^b\delta\,k_x^b+M_y^b\delta\,k_y^b\right.\\&+M_{xy}^b\delta\,k_{xy}^b+M_x^s\delta\,k_x^s+M_y^s\delta\,k_y^s+M_{xy}^s\delta\,k_{xy}^s+S_{yz}^s\delta\,\gamma_{yz}^s\\&\left.+S_{xz}^s\delta\,\gamma_{xz}^s\quad\right]d\Omega-\int_{\Omega}q\,\delta\,wd\Omega=0\end{aligned} \tag{31}$$

where

$$\begin{Bmatrix}N_x, & N_y, & N_{xy}\\M_x^b, & M_y^b, & M_{xy}^b\\M_x^s, & M_y^s, & M_{xy}^s\end{Bmatrix}=\int_{-h/2}^{h/2}\left(\sigma_x,\sigma_y,\tau_{xy}\right)\begin{Bmatrix}1\\z\\f(z)\end{Bmatrix}dz, \tag{32}$$

$$\left(S_{xz}^s,S_{yz}^s\right)=\int_{-h/2}^{h/2}\left(\tau_{xz},\tau_{yz}\right)g(z)dz. \tag{33}$$

The governing equations of equilibrium can be derived from Eq. (31) by integrating the displacement gradients by parts and setting the coefficients $\delta\,u_0$, $\delta\,v_0$, $\delta\,w_b$ and $\delta\,w_s$ zero separately. Thus, one can obtain the equilibrium equations associated with the present shear deformation theory

$$\begin{aligned}\delta\,u\text{:}\quad&\frac{\partial N_x}{\partial x}+\frac{\partial N_{xy}}{\partial y}=0\\\delta\,v\text{:}\quad&\frac{\partial N_{xy}}{\partial x}+\frac{\partial N_y}{\partial y}=0\\\delta\,w_b\text{:}\quad&\frac{\partial^2 M_x^b}{\partial x^2}+2\frac{\partial^2 M_{xy}^b}{\partial x\partial y}+\frac{\partial^2 M_y^b}{\partial y^2}+q=0\\\delta\,w_s\text{:}\quad&\frac{\partial^2 M_x^s}{\partial x^2}+2\frac{\partial^2 M_{xy}^s}{\partial x\partial y}+\frac{\partial^2 M_y^s}{\partial y^2}+\frac{\partial S_{xz}^s}{\partial x}+\frac{\partial S_{yz}^s}{\partial y}+q=0\end{aligned} \tag{34}$$

Using Eq. (27) in Eqs. (32) and (33), the stress resultants of a sandwich plate made up of three layers can be related to the total strains by

$$\begin{Bmatrix}N\\M^b\\M^s\end{Bmatrix}=\begin{bmatrix}A & B & B^s\\A & D & D^s\\B^s & D^s & H^s\end{bmatrix}\begin{Bmatrix}\varepsilon\\k^b\\k^s\end{Bmatrix},\quad S=A^s\gamma, \tag{35}$$

where

$$N=\left\{N_x,N_y,N_{xy}\right\}^t,\quad M^b=\left\{M_x^b,M_y^b,M_{xy}^b\right\}^t,\quad M^s=\left\{M_x^s,M_y^s,M_{xy}^s\right\}^t, \tag{36}$$

$$\varepsilon = \{\varepsilon_x^0, \varepsilon_y^0, \gamma_{xy}^0\}^t, \quad k^b = \{k_x^b, k_y^b, k_{xy}^b\}^t, \quad k^s = \{k_x^s, k_y^s, k_{xy}^s\}^t, \tag{37}$$

$$A = \begin{bmatrix} A_{11} & A_{12} & 0 \\ A_{12} & A_{22} & 0 \\ 0 & 0 & A_{66} \end{bmatrix}, \quad B = \begin{bmatrix} B_{11} & B_{12} & 0 \\ B_{12} & B_{22} & 0 \\ 0 & 0 & B_{66} \end{bmatrix}, \quad D = \begin{bmatrix} D_{11} & D_{12} & 0 \\ D_{12} & D_{22} & 0 \\ 0 & 0 & D_{66} \end{bmatrix}, \tag{38}$$

$$B^s = \begin{bmatrix} B_{11}^s & B_{12}^s & 0 \\ B_{12}^s & B_{22}^s & 0 \\ 0 & 0 & B_{66}^s \end{bmatrix}, \quad D^s = \begin{bmatrix} D_{11}^s & D_{12}^s & 0 \\ D_{12}^s & D_{22}^s & 0 \\ 0 & 0 & D_{66}^s \end{bmatrix}, \quad H^s = \begin{bmatrix} H_{11}^s & H_{12}^s & 0 \\ H_{12}^s & H_{22}^s & 0 \\ 0 & 0 & H_{66}^s \end{bmatrix}, \tag{39}$$

$$S = \{S_{xz}^s, S_{yz}^s\}^t, \qquad \gamma = \{\gamma_{xz}, \gamma_{yz}\}^t, \qquad A^s = \begin{bmatrix} A_{44}^s & 0 \\ 0 & A_{55}^s \end{bmatrix}, \tag{40}$$

where A_{ij}, B_{ij}, etc., are the plate stiffness, defined by

$$\begin{Bmatrix} A_{11} & B_{11} & D_{11} & B_{11}^s & D_{11}^s & H_{11}^s \\ A_{12} & B_{12} & D_{12} & B_{12}^s & D_{12}^s & H_{12}^s \\ A_{66} & B_{66} & D_{66} & B_{66}^s & D_{66}^s & H_{66}^s \end{Bmatrix} = \int_{-h/2}^{h/2} Q_{11}(1, z, z^2, f(z), z\,f(z), f^2(z)) \begin{Bmatrix} 1 \\ \nu \\ \frac{1-\nu}{2} \end{Bmatrix} dz \tag{41}$$

and

$$(A_{22}, B_{22}, D_{22}, B_{22}^s, D_{22}^s, H_{22}^s) = (A_{11}, B_{11}, D_{11}, B_{11}^s, D_{11}^s, H_{11}^s) \tag{42}$$

$$A_{44}^s = A_{55}^s = \int_{h_{n-1}}^{h_n} Q_{44}[g(z)]^2 dz, \tag{43}$$

Substituting from Eq. (35) into Eq. (34), we obtain the following equation

$$\begin{aligned} &A_{11}d_{11}u_0 + A_{66}d_{22}u_0 + (A_{12} + A_{66})d_{12}v_0 - B_{11}d_{111}w_b \\ &-(B_{12} + 2B_{66})d_{122}w_b - (B_{12}^s + 2B_{66}^s)d_{122}w_s - B_{11}^s d_{111}w_s = 0, \end{aligned} \tag{44}$$

$$\begin{aligned} &A_{22}d_{22}v_0 + A_{66}d_{11}v_0 + (A_{12} + A_{66})d_{12}u_0 - B_{22}d_{222}w_b \\ &-(B_{12} + 2B_{66})d_{112}w_b - (B_{12}^s + 2B_{66}^s)d_{112}w_s - B_{22}^s d_{222}w_s = 0, \end{aligned} \tag{45}$$

$$\begin{aligned} &B_{11}d_{111}u_0 + (B_{12} + 2B_{66})d_{122}u_0 + (B_{12} + 2B_{66})d_{112}v_0 + B_{22}d_{222}v_0 \\ &-D_{11}d_{1111}w_b - 2(D_{12} + 2D_{66})d_{1122}w_b - D_{22}d_{2222}w_b - D_{11}^s d_{1111}w_s \\ &-2(D_{12}^s + 2D_{66}^s)d_{1122}w_s - D_{22}^s d_{2222}w_s = q \end{aligned} \tag{46}$$

$$\begin{aligned} &B_{11}^s d_{111}u_0 + (B_{12}^s + 2B_{66}^s)d_{122}u_0 + (B_{12}^s + 2B_{66}^s)d_{112}v_0 + B_{22}^s d_{222}v_0 \\ &-D_{11}^s d_{1111}w_b - 2(D_{12}^s + 2D_{66}^s)d_{1122}w_b - D_{22}^s d_{2222}w_b - H_{11}^s d_{1111}w_s \\ &-2(H_{12}^s + 2H_{66}^s)d_{1122}w_s - H_{22}^s d_{2222}w_s + A_{55}^s d_{11}w_s + A_{44}^s d_{22}w_s = q \end{aligned} \tag{47}$$

where d_{ij}, d_{ijl} and d_{ijlm} are the following differential operators

$$d_{ij} = \frac{\partial^2}{\partial x_i \partial x_j}, \; d_{ijl} = \frac{\partial^3}{\partial x_i \partial x_j \partial x_l}, \; d_{ijlm} = \frac{\partial^4}{\partial x_i \partial x_j \partial x_l \partial x_m}, \; d_i = \frac{\partial}{\partial x_i}, \; (i, j, l, m = 1,2). \tag{48}$$

Exact solution for a simply-supported FGM plate:

Rectangular plates are generally classified in accordance with the type of support used. We are here concerned with the exact solution of Eqs. (44)-(47) for a simply supported FG plate. The following boundary conditions are imposed at the side edges

$$v_0 = w_b = w_s = \frac{\partial w_s}{\partial y} = N_x = M_x^b = M_x^s = 0 \quad \text{at} \quad \text{x = -a/2 , a/2} \tag{49}$$

$$u_0 = w_b = w_s = \frac{\partial w_s}{\partial x} = N_y = M_y^b = M_y^s = 0 \quad \text{at} \quad \text{y = -b/2 , b/2} \tag{50}$$

To solve this problem, Navier assumed that the transverse mechanical and temperature loads, q in the form of a double trigonometric series as

$$q = q_0 \sin(\lambda x) \sin(\mu y) \tag{51}$$

where $\lambda = m\pi/a$, $\mu = n\pi/b$, and q_0 represents the intensity of the load at the plate center.

Following the Navier solution procedure, we assume the following solution form for u_0, v_0, w_b and w_s that satisfies the boundary conditions (Baferani *et al*. 2011, Ait Atmane. 2019, Tounsi *et al*. 2020)

$$\begin{Bmatrix} u_0 \\ v_0 \\ w_b \\ w_s \end{Bmatrix} = \sum_{m=1}^{\infty} \sum_{n=1}^{\infty} \begin{Bmatrix} U_{mn} \cos(\lambda x) \sin(\mu y). e^{i\omega t} \\ V_{mn} \sin(\lambda x) \cos(\mu y). e^{i\omega t} \\ W_{bmn} \sin(\lambda x) \sin(\mu y). e^{i\omega t} \\ W_{smn} \sin(\lambda x) \sin(\mu y). e^{i\omega t} \end{Bmatrix} \tag{52}$$

Where: $\lambda = m\pi/a$, $\mu = n\pi/b$ and ω is the natural frequency and U_{mn}, V_{mn}, W_{bmn} and W_{smn} are arbitrary parameters to be determined subjected to the condition that the solution in Eq. (52) satisfies governing Eqs. (44)-(47). Eq. (52) reduces the governing equations for vibration analysis, one obtains the following operator equation

$$([C] - \omega[G])\{\Delta\} = \{0\}, \tag{53}$$

where $\{\Delta\} = \{U_{mn}, V_{mn}, W_{bmn}, W_{s_{mn}}\}^t$, [C] and [G] refers to the flexural stiffness and mass matrices and ω to the corresponding frequency.

$$[C] = \begin{bmatrix} a_{11} & a_{12} & a_{13} & a_{14} \\ a_{12} & a_{22} & a_{23} & a_{24} \\ a_{13} & a_{23} & a_{33} & a_{34} \\ a_{14} & a_{24} & a_{34} & a_{44} \end{bmatrix}, \qquad [G] = \begin{bmatrix} m_{11} & 0 & 0 & 0 \\ 0 & m_{22} & 0 & 0 \\ 0 & 0 & m_{33} & m_{34} \\ 0 & 0 & m_{34} & m_{44} \end{bmatrix} \tag{54}$$

in which

$$\begin{gathered} a_{11} = A_{11}\lambda^2 + A_{66}\mu^2 \\ a_{12} = \lambda\,\mu\,(A_{12} + A_{66}) \\ a_{13} = -\lambda\,[B_{11}\lambda^2 + (B_{12} + 2B_{66})\,\mu^2] \\ a_{14} = -\lambda\,[B_{11}^s\lambda^2 + (B_{12}^s + 2B_{66}^s)\,\mu^2] \\ a_{22} = A_{66}\lambda^2 + A_{22}\mu^2 \\ a_{23} = -\mu\,[(B_{12} + 2B_{66})\,\lambda^2 + B_{22}\mu^2] \\ a_{24} = -\mu\,[(B_{12}^s + 2B_{66}^s)\,\lambda^2 + B_{22}^s\mu^2] \\ a_{33} = D_{11}\lambda^4 + 2(D_{12} + 2D_{66})\lambda^2\mu^2 + D_{22}\mu^4 \\ a_{34} = D_{11}^s\lambda^4 + 2(D_{12}^s + 2D_{66}^s)\lambda^2\,\mu^2 + D_{22}^s\,\mu^4 \\ a_{44} = H_{11}^s\lambda^4 + 2(H_{11}^s + 2H_{66}^s)\lambda^2\mu^2 + H_{22}^s\mu^4 + A_{55}^s\lambda^2 + A_{44}^s\mu^2 \qquad m_{11} = m_{22} = I_1 \\ m_{33} = I_1 + I_3(\lambda^2 + \mu^2) \\ m_{34} = I_1 + I_5(\lambda^2 + \mu^2) \\ m_{44} = I_1 + I_6(\lambda^2 + \mu^2) \end{gathered} \tag{55}$$

Table 2 Material properties used in the FG plate

Properties	Metal	Ceramic	
	Aluminum (Al)	Zirconia (ZrO_2)	Alumina (Al_2O_3)
E (GPa)	70	200	380
ρ (kg/m^3)	2702	5700	3800

Table 3 Comparison of the fundamental frequency $\bar{\omega} = \omega\, a^2\sqrt{\rho_0 h/G}$ of a rectangular plate $k = 1,\ \alpha = 0$ and $E_{11} = E_{22} = \rho_{11} = \rho_{22} = 1$ (homogeneous materials)

b/a	*h/a*	Hosseini (2011a)	Present
0.5	0.01	49.3032	49.3031
	0.1	45.4869	45.4895
2	0.01	12.3342	12.3341
	0.1	12.0675	12.0676

where

$$(I_1, I_2, I_3, I_4, I_5, I_6) = \int_{-h/2}^{h/2} (1, z, z^2, f(z), zf(z), [f(z)]^2)\rho(z)dz \tag{56}$$

$$\rho(z) = (\rho_C - \rho_m)(\frac{z}{h} + \frac{1}{2})^k + \rho_m \tag{57}$$

4. Numerical results and discussion

In this section, various numerical examples are presented and discussed to verify the accuracy of the present theory in predicting the frequency of simply supported FG plates based on the neutral surface concept.

For verification purpose, the obtained results are compared with those reported in the literature. An (Al/Al_2O_3) or (Al/ZrO_2) plate composed of aluminum (as metal) and alumina or Zirconia (as ceramic) is considered. The material properties assumed in the present analysis are shown in Table 2. Poisson's ratio is 0.3 for both alumina and aluminum. The bottom surfaces of the FG plate are aluminum rich, whereas the top surfaces of the FG plate are alumina or Zirconia rich. To validate the accuracy of the results, the comparisons between the present theory and the available results obtained by Hosseini *et al*. (2011a) in Table 3.

The first example represents the comparison of the fundamental frequency $\bar{\omega} = \omega\, a^2\sqrt{\rho_0 h/G}$ for a rectangular plate with a homogeneous material. It is to be noted that the present results of the fundamental frequency compare very well with the other theory solution for perfect FG plate. For the sake of validation, some results are tabulated here as a comparison with the available ones in the literature. Tables 4(a) and 4(b) shows the comparison of the fundamental frequency parameter $\overline{\beta} = \omega h\sqrt{\rho_m/E_m}$ for SSSS (Al/ZrO_2) square plates with three values of the thickness-to-length ratio ($a/h = 5, 10$ and 20) and for different case of porosity distribution rate. The power law index is taken as $k = 1$. It is to be noted that also the present results of the fundamental frequency

Table 4(a) Comparison of the fundamental frequency $\overline{\beta} = \omega h\sqrt{\rho_m/E_m}$ of a square plate (Al/ZrO_2) with k=1

a/h	Theory		Porosity	
			$\alpha = 0.1$	$\alpha = 0.2$
5	Benyoucef *et al*. (2016)		0.2258	0.2231
	Present method	Type I	0.2186	0.2186
		Type II	0.2276	0.2377
		Type III	0.2282	0.2391
		Type IV	0.2270	0.2364
		Type V	0.2291	0.2411
		Type VI	0.2261	0.2344
10	Benyoucef *et al*. (2016)		0.0612	0.0604
	Present method	Type I	0.0591	0.0591
		Type II	0.0618	0.0649
		Type III	0.0620	0.0654
		Type IV	0.0616	0.0645
		Type V	0.0623	0.0660
		Type VI	0.0613	0.0638
20	Benyoucef *et al*. (2016)		0.0156	0.0157
	Present method	Type I	0.0151	0.0151
		Type II	0.0158	0.0166
		Type III	0.0158	0.0167
		Type IV	0.0157	0.0165
		Type V	0.0159	0.0169
		Type VI	0.0157	0.0163

compare very well with the other theories solution for perfect FG plate (α=0), so we can note that the variation in the porosity distribution rate has a significant effect on the results because the variation of the latter influences the rigidity of the plate.

The example presented in Table 5 show a comparison of non-dimensional fundamental frequency $\overline{\omega} = \omega h\sqrt{\rho_m/E_m}$ of (Al/ZrO_2) square plate for different values of thickness ratio a/h and power law index k, the porosity in the example is taken $\alpha = 0.2$. The fundamental frequency parameter ω is obtained using the present theory (NFSDT) and compared with those 3-D exact solutions of Batra *et al* (2004), higher shear deformation theories (HSDT) with 2-D higher order theory solutions of Matsunaga *et al* (2008), Reddy's theory with analytical method solutions of Hosseini *et al*. (2011b).

In Table 6, the non-dimensional frequencies $\widehat{\omega} = \omega h\sqrt{\rho_c/E_c}$ of thin and thick (Al/Al_2O_3) square plates with thickness ratio varying between (5, 10 and 20) and the power law index varying from (0.5, 1, 4, 10) are investigated, the results obtained by the present theory are presented in this table and compared to those predicted by TSDT (Ait Atmane *et al* 2019), FSDT (Draiche *et al* 2019) and Tounsi *et al* (2020). We note that $\alpha = 0.2$ in this example. It can be seen that the results obtained by present theory are in good agreement with the other theories solution for perfect FG plate (Type I, $\alpha = 0$). Il can also noticed that the frequencies decreases as the FG plate becomes richer in metal.

Table 4(b) Variation of fundamental frequency of square FG plate with k and a/h ratio for SSSS boundary condition, $\alpha = 0.1$

a/h	Methods		Power law index				
			0	1	2	5	10
10	Firooz Bakhtiari-Nejad (2015)		1.7748	1.4764	1.4628	1.4106	1.3711
	Present	Type I	1.7684	1.4889	1.4339	1.3722	1.3350
		Type II	1.7687	1.5195	1.4569	1.4008	1.3638
		Type III	1.7835	1.5323	1.4687	1.4113	1.3738
		Type IV	1.7542	1.5070	1.4453	1.3905	1.3540
		Type V	1.8065	1.5521	1.4869	1.4273	1.3890
		Type VI	1.7332	1.4888	1.4284	1.3753	1.3394
10	Firooz Bakhtiari-Nejad (2015)		1.9339	1.6583	1.5968	1.5491	1.5066
	Present	Type I	1.9317	1.6183	1.5658	1.5072	1.4662
		Type II	1.9351	1.6601	1.5997	1.5495	1.5084
		Type III	1.9530	1.6761	1.6151	1.5643	1.5229
		Type IV	1.9176	1.6445	1.5846	1.5350	1.4943
		Type V	1.9810	1.7010	1.6392	1.5874	1.5453
		Type VI	1.8922	1.6219	1.5628	1.5140	1.4737
20	Firooz Bakhtiari-Nejad (2015)		1.9570	1.6999	1.6401	1.5937	1.5491
	Present	Type I	1.9821	1.6579	1.6065	1.5494	1.5071
		Type II	1.9865	1.7035	1.6442	1.5966	1.5541
		Type III	2.0056	1.7206	1.6610	1.6130	1.5703
		Type IV	1.9680	1.6868	1.6279	1.5806	1.5385
		Type V	2.0352	1.7473	1.6871	1.6387	1.5954
		Type VI	1.9412	1.6628	1.6044	1.5575	1.5159
100	Firooz Bakhtiari-Nejad (2015)		1.9974	1.7117	1.6552	1.6062	1.5652
	Present	Type I	1.9992	1.67136	1.6204	1.5638	1.5212
		Type II	2.0041	1.71832	1.6595	1.6128	1.5699
		Type III	2.0235	1.7358	1.6767	1.6298	1.5866
		Type IV	1.9852	1.7013	1.6428	1.5963	1.5537
		Type V	2.0538	1.7631	1.7036	1.6564	1.6127
		Type VI	1.9579	1.6767	1.6186	1.5724	1.5303

Table 5 Comparison of non-dimensional fundamental frequency $\bar{\omega} = \omega h\sqrt{\rho_m/E_m}$ of (Al/ZrO_2) square plate $\alpha = 0.2$

Methods		k=1			a/h=5		
		a/h=5	a/h=10	a/h=20	k=2	k=3	k=5
3-D (Batra *et al*. 2004)		0.2192	0.0596	0.0153	0.2197	0.2211	0.2225
HSDT (Matsunaga *et al*. 2008)		0.2285	0.0619	0.0158	0.2264	0.227	0.2281
HSDT (Hosseini *et al*. 2011b)		0.2276	0.0619	0.0158	0.2256	0.2263	0.2272
Present	Type I	0.2186	0.0591	0.0151	0.2188	0.2185	0.2176
	Type II	0.2377	0.0649	0.0166	0.2406	0.2401	0.2388
	Type III	0.2391	0.0654	0.0167	0.2421	0.2414	0.2399
	Type IV	0.2364	0.0645	0.0165	0.2391	0.2387	0.2377
	Type V	0.2411	0.0660	0.0169	0.2443	0.2433	0.2414
	Type VI	0.2344	0.0638	0.0163	0.2368	0.2366	0.2358

Table 6 Comparison of natural frequency parameter $\hat{\omega} = \omega h\sqrt{\rho_c/E_c}$ of (Al/Al_2O_3) square plate. $\alpha = 0.2$

a/h	Mode (*m*,*n*)	Methods		Power law index			
				k=0.5	*k*=1	*k*=4	*k*=10
5	(1,1)	TSDT (Air Atmane *et al.* 2019)		0.2113	0.1631	0.1378	0.1301
		FSDT (Draiche *et al*. 2019)		0.2112	0.1631	0.1397	0.1324
		Tounsi *et al.* (2020)		0.2112	0.1631	0.1397	0.1324
		Present	Type I	0.2112	0.1461	0.1261	0.1146
			Type II	0.2294	0.1556	0.1289	0.1106
			Type II	0.2298	0.1549	0.1265	0.1065
			Type IV	0.2290	0.1563	0.1309	0.1141
			Type V	0.2304	0.1536	0.1221	0.0964
			Type VI	0.2284	0.1571	0.1334	0.1182
	(1,2)	TSDT (Air Atmane *et al.* 2019)		0.4623	0.3607	0.2980	0.2771
		FSDT (Draiche *et al*. 2019)		0.4618	0.3604	0.3049	0.2856
		Tounsi *et al.* (2020)		0.4618	0.3604	0.3049	0.2856
		Present	Type I	0.4623	0.3281	0.2767	0.2493
			Type II	0.4975	0.3466	0.2733	0.2255
			Type II	0.4977	0.3446	0.2664	0.2126
			Type IV	0.4973	0.3485	0.2793	0.2360
			Type V	0.4978	0.3410	0.2541	0.1852
			Type VI	0.4970	0.3509	0.2870	0.2487
10	(1,1)	TSDT (Air Atmane *et al.* 2019)		0.0577	0.0442	0.0381	0.0364
		FSDT (Draiche *et al*. 2019)		0.0577	0.0442	0.0382	0.0366
		Tounsi *et al.* (2020)		0.0577	0.0442	0.0382	0.0366
		Present	Type I	0.0576	0.0391	0.0344	0.0315
			Type II	0.0631	0.0419	0.0364	0.0325
			Type II	0.0633	0.0418	0.0360	0.0319
			Type IV	0.0629	0.0420	0.0367	0.0330
			Type V	0.0636	0.0415	0.0353	0.0305
			Type VI	0.0626	0.0422	0.0371	0.0335
	(1,2)	TSDT (Air Atmane *et al.* 2019)		0.1377	0.1059	0.0903	0.0856
		FSDT (Draiche *et al*. 2019)		0.1376	0.1059	0.0911	0.0867
		Tounsi *et al.* (2020)		0.1376	0.1059	0.0911	0.0867
		Present	Type I	0.1376	0.0943	0.0821	0.0821
			Type II	0.1500	0.1008	0.0852	0.0743
			Type II	0.1503	0.1004	0.0839	0.0720
			Type IV	0.1496	0.1012	0.0863	0.0761
			Type V	0.1508	0.0996	0.0815	0.0667
			Type VI	0.1491	0.1016	0.0876	0.0783
20	(1,1)	TSDT (Air Atmane *et al.* 2019)		0.0148	0.0113	0.0098	0.0094
		FSDT (Draiche *et al*. 2019)		0.0148	0.0113	0.0098	0.0094
		Tounsi *et al.* (2020)		0.0148	0.0113	0.0098	0.0094
		Present	Type I	0.0147	0.0099	0.0088	0.0081
			Type II	0.01624	0.0107	0.00947	0.00858
			Type II	0.01629	0.0106	0.00940	0.00851
			Type IV	0.01618	0.0107	0.00953	0.00865
			Type V	0.01637	0.0106	0.00927	0.00838
			Type VI	0.01610	0.0107	0.00959	0.00873

Table 7 Comparison of non-dimensional fundamental frequency $\bar{\omega} = \omega h\sqrt{\rho_m/E_m}$ of (Al/Al_2O_3) square plate $a = 20h$ and $\alpha = 0.2$ (elastic foundation case)

k	k_0	k_1	Methods							
			Baferani (2011)	Tai (2012)	Present					
					Type I	Type II	Type III	Type IV	Type V	Type VI
1	0	0	0.0227	0.0222	0.0196	0.02107	0.02101	0.02113	0.02088	0.02120
	0	100	0.0382	0.0378	0.0356	0.03917	0.03922	0.03911	0.03929	0.03902
	100	0	0.0238	0.0233	0.0207	0.02240	0.02234	0.02244	0.02224	0.02249
	100	100	0.0388	0.0384	0.0362	0.03984	0.03990	0.03978	0.03996	0.03968
2	0	0	0.0209	0.0202	0.0186	0.02055	0.02058	0.02052	0.02062	0.02047
	0	100	0.0380	0.0374	0.0355	0.03942	0.03948	0.03935	0.03955	0.03923
	100	0	0.0221	0.0214	0.0198	0.02199	0.02203	0.02195	0.02208	0.02189
	100	100	0.0381	0.0386	0.0361	0.04009	0.04015	0.04002	0.04022	0.03990
5	0	0	0.0197	0.0191	0.0169	0.01801	0.01784	0.01816	0.01751	0.01834
	0	100	0.0381	0.0377	0.0350	0.03778	0.03746	0.03801	0.03673	0.03825
	100	0	0.0210	0.0205	0.0184	0.01971	0.01955	0.01985	0.01924	0.02000
	100	100	0.0388	0.0384	0.0356	0.03841	0.03807	0.03866	0.03731	0.03890

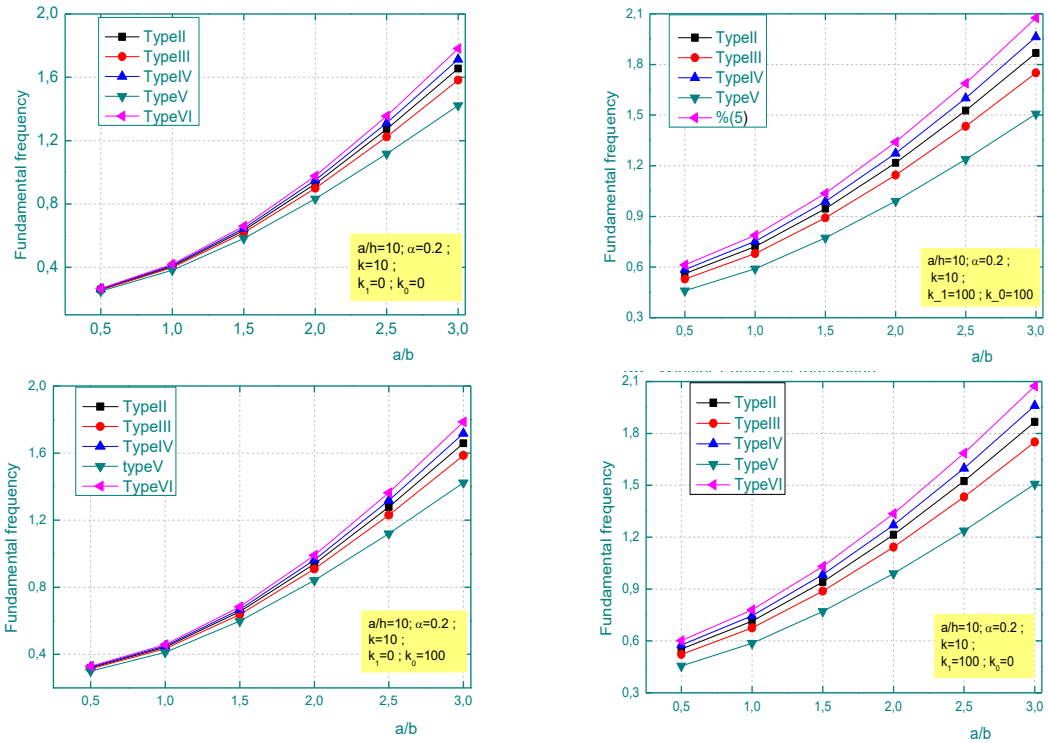

Fig. 2 Comparison of non-dimensional fundamental frequency $\bar{\omega}$ of Al/Al_2O_3 square FG plate versus ratio *a/b* (a) without elastic foundation, (b) Winkler-Pasternak foundation, (c) Winkler elastic foundation (d) Pasternak elastic foundation

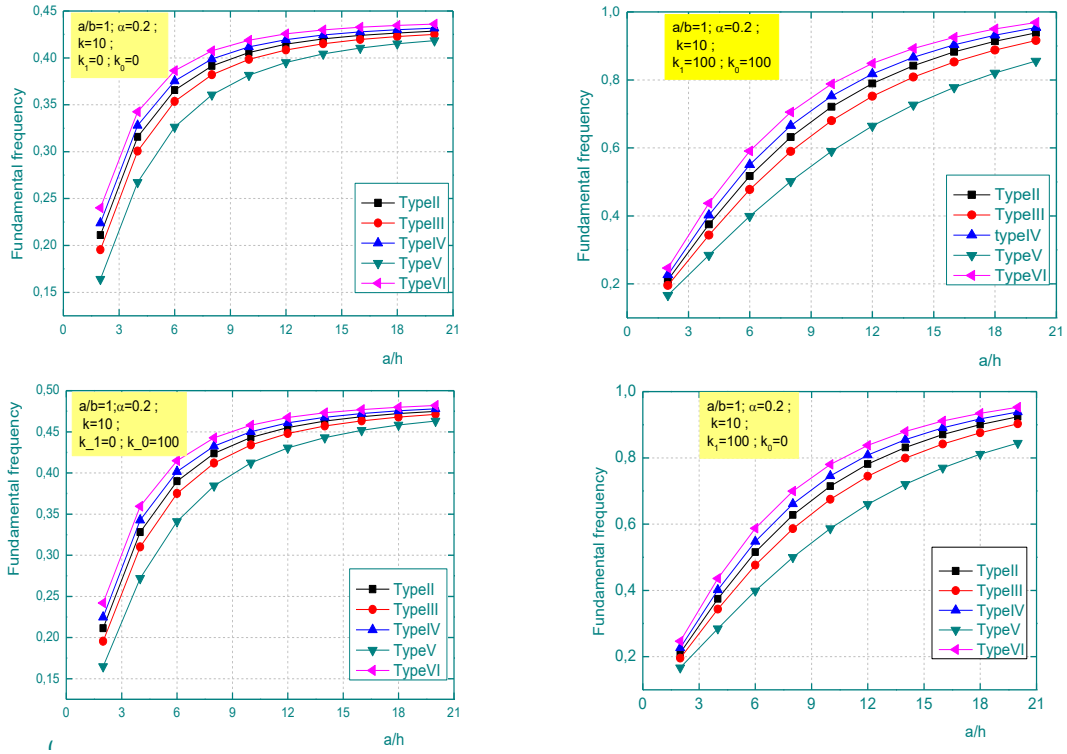

Fig. 3 Comparison of non-dimensional fundamental frequency $\bar{\omega}$ of Al/Al_2O_3 square FG plate versus thickness ratio *a/h* (a) without elastic foundation, (b) Winkler-Pasternak foundation, (c) Winkler elastic foundation (d) Pasternak elastic foundation

Tables 7 and 8 show the comparison of fundamental frequency of FG rectangular plates on their elastic foundation with those reported by Baferani *et al* (2011), Tai *et al* (2012) and Kaci *et al*. (2020) with different values of the thickness-to-length ratios, foundation stiffness parameters and porosity distribution rate, the results for the case of (Type I) are in good agreement with each other.

The dimensionless fundamental frequency as a function of the aspect ratio (a/b), side-to-thickness ratio (a/h) and power law index (k) of porous FGM plate for different variation of porosity distribution rate are illustrated in Figs. 2, Fig. 3 and Fig. 4, respectively. In each figure we present four cases of elastic foundation. (a) without elastic foundation, (b) winkler-pasternak foundation, (c) winkler elastic foundation and (d) pasternak elastic foundation.

It can be seen that the dimensionless fundamental frequency increase as the aspect ratio a/b and the side-to-thickness ratio a/h increase (Figs. 2 and 3) because the FG plaque becomes thinner. Also, the case of FG plate Winkler-Pasternak foundation and Pasternak elastic foundation gives the largest value of frequency. The (Type VI) of the variation in the porosity distribution rate in FG plate gives the largest value of frequency while the (Type V) gives the smallest ones.

From the Fig. 4 we can observe that the dimensional fundamental frequency decreases when the power law index k increase. At the same we noticed that the largest value of the fundamental frequency can be determinate with Winkler-Pasternak elastic foundation and Pasternak elastic foundation. The variation in the porosity distribution rate in FG plate (Type V) gives the smallest value of frequency while the (Type VI) gives the largest ones, because the existence of maximum

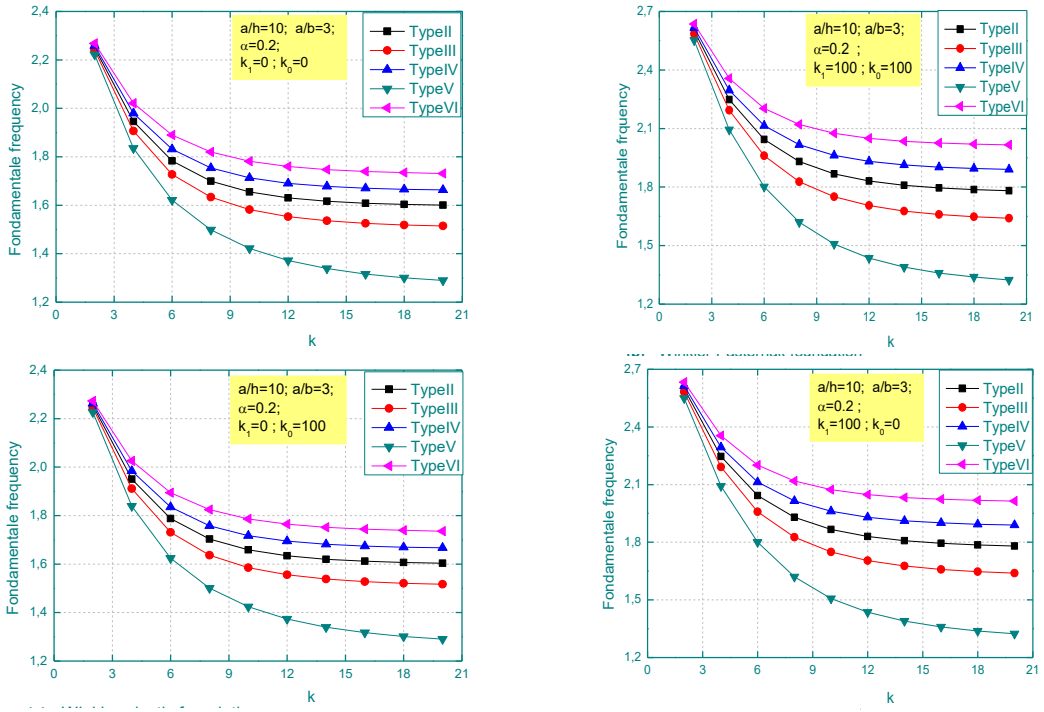

Fig. 4 Comparison of non-dimensional fundamental frequency $\bar{\omega}$ of Al/Al_2O_3 rectangular FG plate versus power law index k (a) without elastic foundation, (b) Winkler-Pasternak foundation, (c) Winkler elastic foundation (d) Pasternak elastic foundation

Table 8 Non-dimensional fundamental frequency $\bar{\omega} = \omega\, a^2\sqrt{\rho_m/E_m}$ of SS plate (Al/Al_2O_3) $k = 2$ and $\alpha = 0.2$

k_0	k_1	a/b	a/h	Theory						
				Kaci (2020)	Present					
					Type I	Type II	Type III	Type IV	Type V	Type VI
0	0	1	10	7.8763	7.2802	7.9936	7.9944	7.9912	7.9920	7.9846
			20	8.0749	7.4433	8.2229	8.2346	8.2108	8.2514	8.1917
		2	10	18.8206	17.4798	19.0036	18.9663	19.0327	18.8929	19.0633
			20	19.9333	18.4000	20.2627	20.2774	20.2452	20.2939	20.2139
0	100	1	10	14.7799	13.0765	14.1340	14.0863	14.1727	13.9950	14.2165
			20	14.9549	14.2220	15.7684	15.7929	15.7408	15.8221	15.6944
		2	10	27.1506	23.6168	25.3013	25.1762	25.4082	24.9488	25.5391
			20	28.1214	26.2529	28.9289	28.9421	28.9078	28.9441	28.8635
100	0	1	10	8.3643	7.7494	8.5132	8.5141	8.5103	8.5112	8.5026
			20	8.5576	7.94972	8.7974	8.8120	8.7823	8.8331	8.7585
		2	10	19.0258	17.6501	19.1856	19.1472	19.2158	19.0715	19.2475
			20	20.1323	18.6012	20.4887	20.5041	20.4704	20.5214	20.4379
100	100	1	10	15.0455	13.2655	14.3235	14.2724	14.3653	14.1752	14.4131
			20	15.2209	14.4684	16.0371	16.0609	16.0098	16.0888	15.9638
		2	10	27.2931	23.7083	25.3911	25.2640	25.4999	25.0332	25.6331
			20	28.2628	26.3815	29.0683	29.0809	29.0475	29.0819	29.0036

porosity in the ceramic significantly reduces the rigidity of the plate.

5. Conclusions

In this work, an efficient new refined shear deformation theory based on the middle surface concept was effectively used to study extensively the free vibration analysis of porous FG plates simply-supported resting on elastic foundations using an analytical procedure. The modified rule of mixture, covering different variation of porosity distribution rate is used to describe and approximate material properties of the imperfect FG plates. In accordance with numerical results, some conclusions can be drawn as follows:

- The fundamental frequencies become more important when the variation of distribution rate of porosity is of type VI.
- The largest value of the fundamental frequency can be determinate with Winkler-Pasternak elastic foundation and Pasternak elastic foundation.
- The frequencies decreases as the FG plate becomes richer in metal.

Acknowledgments

This research was supported by the Algerian Ministry of Higher Education and Scientific Research (MESRS) as part of the grant for the PRFU research project n° A01L02UN140120200002 and by the University of Tiaret, in Algeria.

References

Abbès, B., Benhenni, M.A., Daouadji, T.H., Abbes, F., Adim, B. and Li, Y. (2019), "Numerical analysis for free vibration of hybrid laminated composite plates for different boundary conditions", *Struct. Eng. Mech.*, **70**(5), 535-549. https://doi.org/10.12989/sem.2019.70.5.535.

Abdelhak, Z., Hadji, L., Daouadji, T.H. and Adda Bedia, E.A. (2016), "Thermal buckling response of functionally graded sandwich plates with clamped boundary conditions", *Smart Struct. Syst.*, **18**(2), 267-291. https://doi.org/10.12989/sss.2016.18.2.267.

Adim Belkacem *et al*. (2016b), "Effects of thickness stretching in FGM plates using a quasi-3D higher order shear deformation theory", *Adv. Mater. Res.*, **5**(4), 223-244. https://doi.org/10.12989/amr.2016.5.4.223.

Adim, B., Daouadji, T.H. and Abbes, B. (2016a), "Buckling analysis of anti-symmetric cross-ply laminated composite plates under different boundary conditions", *Int. Appl. Mech.*, **52**(6), 126-141. https://doi.org/10.1007/s10778-016-0787-x.

Adim, B., Daouadji, T.H., Abbes, B. and Rabahi, A. (2016b), "Buckling and free vibration analysis of laminated composite plates using an efficient and simple higher order shear deformation theory", *Mech. Indus.*, **17**, 512. https://doi.org/10.1051/meca/2015112.

Adim, B., Daouadji, T.H., Rabia, B. and Hadji, L. (2016a), "An efficient and simple higher order shear deformation theory for bending analysis of composite plates under various boundary conditions", *Earthq. Struct.*, **11**(1), 63-82. https://doi.org/10.12989/eas.2016.11.1.063.

Aicha, K., Rabia, B., Daouadji, T.H. and Bouzidene, A. (2020), "Effect of porosity distribution rate for bending analysis of imperfect FGM plates resting on Winkler-Pasternak foundations under various boundary conditions", *Couple. Syst. Mech.*, **9**(6), 575-597. http://doi.org/10.12989/csm.2020.9.6.575.

Baferani, A.H., Saidi, A.R. and Ehteshami, H. (2011), "Accurate solution for free vibration analysis of

functionally graded thick rectangular plates resting on elastic foundation", *Compos. Struct.*, **93**(7), 1842-1853. https://doi.org/10.1016/j.compstruct.2011.01.020.

Bakhtiari-Nejad, F., Shamshirsaz, M., Mohammadzadeh, M. and Samie, S. (2014). "Free vibration analysis of FG skew plates based on second order shear deformation theory", *International Design Engineering Technical Conferences and Computers and Information in Engineering Conference*, **46414**, V008T11A024, August. https://doi.org/10.1115/DETC2014-34085.

Batra, R.C. and Vel, S.S. (2004), "Three-dimensional exact solution for the vibration of functionally graded rectangular plates", *J. Sound Vib.*, **272**(3-5), 703-730. http://doi.org/10.1016/S0022-460X(03)00412-7.

Belabed, Z., Houari, M.S.A., Tounsi, A., Mahmoud, S.R. and Bég, O.A. (2014), "An efficient and simple higher order shear and normal deformation theory for functionally graded material (FGM) plates", *Compos.: B Eng.*, **60**, 274-283. https://doi.org/10.1016/j.compositesb.2013.12.057.

Belkacem, A., Tahar, H.D., Abderrezak, R., Amine, B.M., Mohamed, Z. and Boussad, A. (2018), "Mechanical buckling analysis of hybrid laminated composite plates under different boundary conditions", *Struct. Eng. Mech.*, **66**(6), 761-769. https://doi.org/10.12989/sem.2018.66.6.761.

Benferhat, R., Daouadji, T.H. and Abderezak, R. (2021), "Effect of porosity on fundamental frequencies of FGM sandwich plates", *Compos. Mater. Eng.*, **3**(1), 25-40. http://doi.org/10.12989/cme.2021.3.1.025.

Benferhat, R., Daouadji, T.H. and Mansour, M.S. (2016a), "Free vibration analysis of FG plates resting on the elastic foundation and based on the neutral surface concept using higher order shear deformation theory", *Comptes Rendus Mecanique*, **344**(9), 631-641. https://doi.org/10.1016/j.crme.2016.03.002.

Benferhat, R., Hassaine Daouadji, T., Said Mansour, M. and Hadji, L. (2016b), "Effect of porosity on the bending and free vibration response of functionally graded plates resting on Winkler-Pasternak foundations", *Earthq. Struct.*, **10**(6), 1429-1449. https://doi.org/10.12989/eas.2016.10.6.1429.

Benhenni, M.A., Daouadji, T.H., Abbes, B., Adim, B., Li, Y. and Abbes, F. (2018), "Dynamic analysis for anti-symmetric cross-ply and angle-ply laminates for simply supported thick hybrid rectangular plates", *Adv. Mater. Res.*, **7**(2), 83-103. https://doi.org/10.12989/amr.2018.7.2.119.

Benyoucef, S., Mouaici, F., Ait Atmane, H. and Tounsi, A. (2016), "Effect of porosity on vibrational characteristics of non-homogeneous plates using hyperbolic shear deformation theory", *Wind Struct.*, **22**(4), 429-454. http://doi.org/10.12989/was.2016.22.4.429.

Bourada, F., Bousahla, A.A., Tounsi, A., Bedia, E.A., Mahmoud, S.R., Benrahou, K.H. and Tounsi, A. (2020), "Stability and dynamic analyses of SW-CNT reinforced concrete beam resting on elastic-foundation", *Comput. Concrete*, **25**(6), 485-495. https://doi.org/10.12989/cac.2020.25.6.485.

Chaabane, L.A. (2019), "Analytical study of bending and free vibration responses of functionally graded beams resting on elastic foundation", *Struct. Eng. Mech.*, **71**(2), 185-196. https://doi.org/10.12989/sem.2019.71.2.185.

Chikr, S.C., Kaci, A., Bousahla, A.A., Bourada, F., Tounsi, A., Bedia, E.A., ... & Tounsi, A. (2020), "A novel four-unknown integral model for buckling response of FG sandwich plates resting on elastic foundations under various boundary conditions using Galerkin's approach", *Geomech. Eng.*, **21**(5), 471-487. https://doi.org/10.12989/gae.2020.21.5.471.

Daouadji, T.H., Benferhat, R. and Adim, B. (2016), "Bending analysis of an imperfect advanced composite plates resting on the elastic foundations", *Couple. Syst. Mech.*, **5**(3), 269-285. http://doi.org/10.12989/csm.2017.5.3.269.

Draiche, K., Bousahla, A.A., Tounsi, A., Alwabli, A.S., Tounsi, A. and Mahmoud, S.R. (2019), "Static analysis of laminated reinforced composite plates using a simple first-order shear deformation theory", *Comput. Concrete*, **24**(4), 369-378. https://doi.org/10.12989/cac.2019.24.4.369.

Feng, H., Shen, D. and Tahouneh, V. (2020), "Vibration analysis of sandwich sector plate with porous core and functionally graded wavy carbon nanotube-reinforced layers", *Steel Compos. Struct.*, **37**(6) 711-731. https://doi.org/10.12989/scs.2020.37.6.711.

Fenjan, R.M., Moustafa, N.M. and Faleh, N.M. (2020), "Scale-dependent thermal vibration analysis of FG beams having porosities based on DQM", *Adv. Nano Res.*, **8**(4) 283-292. https://doi.org/10.12989/anr.2020.8.4.283.

Foroutan, K. and Ahmadi, H. (2020), "Simultaneous resonances of SSMFG cylindrical shells resting on

viscoelastic foundations", *Steel Compos. Struct*., **37**(1), 51-73. https://doi.org/10.12989/scs.2020.37.1.051.
Hadj, B., Rabia, B. and Daouadji, T.H. (2019), "Influence of the distribution shape of porosity on the bending FGM new plate model resting on elastic foundations", *Struct. Eng. Mech.*, **72**(1), 823-832. https://doi.org/10.12989/sem.2019.72.1.061.
Hadj, B., Rabia, B. and Daouadji, T.H. (2021), "Vibration analysis of porous FGM plate resting on elastic foundations: Effect of the distribution shape of porosity", *Couple. Syst Mech.*, **10**(1), 61-77. http://doi.org/10.12989/csm.2021.10.1.061.
Hosseini-Hashemi, S., Fadaee, M. and Atashipour, S.R. (2011a), "Study on the free vibration of thick functionally graded plates according to a new exact closed-form procedure", *Compos. Struct.*, **93**(2), 722-735. https://doi.org/10.1016/j.compstruct.2010.08.007.
Hosseini-Hashemi, S., Fadaee, M.O.H.A.M.M.A.D. and Atashipour, S.R. (2011b), "A new exact analytical approach for free vibration of Reissner-Mindlin functionally graded rectangular plates", *Int. J. Mech. Sci.*, **53**(1), 11-22. https://doi.org/10.1016/j.ijmecsci.2010.10.002.
Huang, C.S., Yang, P.J. and Chang, M.J. (2012), "Three-dimensional vibration analyses of functionally graded material rectangular plates with through internal cracks", *Compos. Struct.*, **94**, 2764-2776. https://doi.org/10.1016/j.compstruct.2012.04.003
Jia, A., Liu, H., Ren, L., Yun, Y. and Tahouneh, V. (2020), "Influence of porosity distribution on vibration analysis of GPLs-reinforcement sectorial plate", *Steel Compos. Struct*., **35**(1), 111-127. https://doi.org/10.12989/scs.2020.35.1.111.
Kaddari, M., Kaci, A., Bousahla, A.A., Tounsi, A., Bourada, F., Bedia, E.A. and Al-Osta, M.A. (2020), "A study on the structural behaviour of functionally graded porous plates on elastic foundation using a new quasi-3D model: Bending and Free vibration analysis", *Comput. Concrete*, **25**(1), 37-57. https://doi.org/10.12989/cac.2020.25.1.037.
Keleshteri Mohammadzadeh, M., Samie-Anarestani, S. and Assadi, A. (2017a), "Large deformation analysis of single-crystalline nanoplates with cubic anisotropy", *Acta Mechanica*, **228**, 3345-3368. https://doi.org/10.1007/s00707-017-1862-z.
Keleshteri, M.M. and Jelovica, J. (2020), "Nonlinear vibration behavior of functionally graded porous cylindrical panels", *Compos. Struct.*, **239**, 112028. https://doi.org/10.1016/j.compstruct.2020.112028.
Keleshteri, M.M. and Jelovica, J. (2021), "Nonlinear vibration analysis of bidirectional porous beams", *Eng. Comput.*, 1-17. https://doi.org/10.1007/s00366-021-01553-x.
Keleshteri, M.M. and Jelovica, J. (2022), "Beam theory reformulation to implement various boundary conditions for generalized differential quadrature method", *Eng. Struct.*, **252**, 113666. https://doi.org/10.1016/j.engstruct.2021.113666.
Keleshteri, M.M., Asadi, H. and Aghdam, M.M. (2019), "Nonlinear bending analysis of FG-CNTRC annular plates with variable thickness on elastic foundation", *Thin Wall. Struct*., **135**, 453-462. https://doi.org/10.1016/j.tws.2018.11.020.
Keleshteri, M.M., Asadi, H. and Wang, Q. (2018), "On the snap-through instability of post-buckled FG-CNTRC rectangular plates with integrated piezoelectric layers", *Comput. Meth. Appl. Mech. Eng.*, **331**(1), 53-71. https://doi.org/10.1016/j.cma.2017.11.015.
Kerr A.D. (1964), "Elastic and viscoelastic foundation models", *ASME J. Appl. Mech*., **31**(3), 491-498. https://doi.org/10.1115/1.3629667.
Lal, R. and Ahlawat, N. (2015), "Axisymmetric vibrations and buckling analysis of functionally graded circular plates via differential transform method", *Eur. J. Mech. A/Solid.*, **52**, 85-94. https://doi.org/10.1016/j.euromechsol.2015.02.004.
Lata, P. and Kaur, H. (2021), "Deformation in a homogeneous isotropic thermoelastic solid with multi-dual-phase-lag heat & two temperature using modified couple stress theory", *Compos. Mater. Eng*., **3**(2), 89-106. https://doi.org/10.12989/cme.2021.3.2.089.
Li, L. and Zhang, D.G (2016), "Free vibration analysis of rotating functionally graded rectangular plates", *Compos. Struct.*, **136**, 493-504. https://doi.org/10.1016/j.compstruct.2015.10.013.
Matsunaga, H. (2008), "Free vibration and stability of functionally graded plates according to a 2-D higher-order deformation theory", *Compos. Struct.*, **82**(4), 499-512.

http://doi.org/10.1016/j.compstruct.2007.01.030.
Mohammad Talha, B.N. (2010), "Singh, Static response and free vibration analysis of FGM plates using higher order shear deformation theory", *Appl. Math. Model*., **34**, 3991-4011. https://doi.org/10.1016/j.apm.2010.03.034.
Mohammadzadeh-Keleshteri, M., Asadi, H. and Aghdam, M.M. (2017b), "Geometrical nonlinear free vibration responses of FG-CNT reinforced composite annular sector plates integrated with piezoelectric layers", *Compos. Struct.*, **171**(1), 100-112. https://doi.org/10.1016/j.compstruct.2017.01.048.
Nebab, M., Atmane, H.A., Bennai, R., Tounsi, A. and Bedia, E.A. (2019), "Vibration response and wave propagation in FG plates resting on elastic foundations using HSDT", *Struct. Eng. Mech.*, **69**(5), 511-525. http://doi.org/10.12989/sem.2019.69.5.511.
Nejadi, M.M. and Mohammadimehr, M. (2020), "Buckling analysis of nano composite sandwich Euler-Bernoulli beam considering porosity distribution on elastic foundation using DQM", *Adv. Nano Res*., **8**(1), 59-68. https://doi.org/10.12989/anr.2020.8.1.059.
Parandvar, H. and Farid, M. (2015), "Nonlinear reduced order modeling of functionally graded plates subjected to random load in thermal environment", *Compos. Struct.*, **126**, 174-183. https://doi.org/10.1016/j.compstruct.2015.02.006.
Parandvar, H. and Farid, M. (2016), "Large amplitude vibration of FGM plates in thermal environment subjected to simultaneously static pressure and harmonic force using multimodal FEM", *Compos. Struct.*, **141**(1), 163-171. https://doi.org/10.1016/j.compstruct.2016.01.044.
Pourmoayed, A., Fard, K.M. and Rousta, B. (2021), "Free vibration analysis of sandwich structures reinforced by functionally graded carbon nanotubes", *Compos. Mater. Eng*., **3**(1), 1-23. https://doi.org/10.12989/cme.2021.3.1.001.
Praveen, G.N. and Reddy, J.N. (1998), "Nonlinear transient thermoelastic analysis of functionally graded ceramic-metal plates", *Int. J. Solid. Struct.*, **35**(33), 4457-4476. https://doi.org/10.1016/S0020-7683(97)00253-9.
Rabia, B., Daouadji, T.H. and Abderezak, R. (2019), "Effect of porosity in interfacial stress analysis of perfect FGM beams reinforced with a porous functionally graded materials plate", *Struct. Eng. Mech.*, **72**(3), 293-304. https://doi.org/10.12989/sem.2019.72.3.293.
Rabia, B., Tahar, H.D. and Abderezak, R. (2020), "Thermo-mechanical behavior of porous FG plate resting on the Winkler-Pasternak foundation", *Couple. Syst Mech.*, **9**(6), 499-519. http://dx.doi.org/10.12989/csm.2020.9.6.499.
Ramu, I. and Mohanty, S.C. (2014), "Modal analysis of Functionally Graded material Plates using Finite Element Method", *Procedia Mater. Sci.*, **6**, 460-467. https://doi.org/10.1016/j.mspro.2014.07.059.
Sator, L., Sladek, V., Sladek, J. and Young, D.L. (2016), "Elastodynamics of FGM plates by mesh-free method", *Compos. Struct.*, **140**, 309-322. https://doi.org/10.1016/j.compstruct.2015.12.065.
Shariati, A., Ebrahimi, F., Karimiasl, M., Vinyas, M. and Toghroli, A. (2020), "On transient hygrothermal vibration of embedded viscoelastic flexoelectric/piezoelectric nanobeams under magnetic loading", *Adv. Nano Res*., **8**(1), 49-58. https://doi.org/10.12989/anr.2020.8.1.049.
Si, H., Shen, D., Xia, J. and Tahouneh, V. (2020), "Vibration behavior of functionally graded sandwich beam with porous core and nanocomposite layers", *Steel Compos. Struct*., **36**(1), 1-16. https://doi.org/10.12989/scs.2020.36.1.001.
Ta, H.D. and Noh, H.C. (2015), "Analytical solution for the dynamic response of functionally graded plates resting on elastic foundation using a refined plate theory", *Appl. Math. Model.*, **39**, 6243-6257. https://doi.org/10.1016/j.apm.2015.01.062.
Taczała, M., Buczkowski, R. and Kleiber, M. (2015), "Postbuckling analysis of functionally graded plates on an elastic foundation", *Compos. Struct.*, **132**, 842-847. https://doi.org/10.1016/j.compstruct.2015.06.055.
Taherifar, R., Zareei, S.A., Bidgoli, M.R. and Kolahchi, R. (2020), "Seismic analysis in pad concrete foundation reinforced by nanoparticles covered by smart layer utilizing plate higher order theory", *Steel Compos. Struct*., **37**(1), 99-115. https://doi.org/10.12989/scs.2020.37.1.099.
Thai, C.H., Zenkour, A.M., Wahab, M.A. and Nguyen-Xuan, H. (2016), "A simple four-unknown shear and normal deformations theory for functionally graded isotropic and sandwich plates based on isogeometric

analysis", *Compos. Struct.*, **139**, 77-95. https://doi.org/10.1016/j.compstruct.2015.11.066.
Thai, H.T. and Choi, D.H. (2012), "A refined shear deformation theory for free vibration of functionally graded plates on elastic foundation", *Compos. Part B: Eng.*, **43**(5), 2335-2347. https://doi.org/10.1016/j.compositesb.2011.11.062.
Thai, H.T. and Kim, S.E. (2013), "Closed-form solution for buckling analysis of thick functionally graded plates on elastic foundation", *Int. J. Mech. Sci.*, **75**, 34-44. http://doi.org/10.1016/j.ijmecsci.2013.06.007.
Tlidji, Y., Benferhat, R. and Tahar, H.D. (2021a), "Study and analysis of the free vibration for FGM microbeam containing various distribution shape of porosity", *Struct. Eng. Mech.*, **77**(2), 217-229. http://doi.org/10.12989/sem.2021.77.2.217.
Tlidji, Y., Benferhat, R., Trinh, L.C., Tahar, H.D. and Abdelouahed, T. (2021b), "New state-space approach to dynamic analysis of porous FG beam under different boundary conditions", *Adv. Nano Res.*, **11**(4), 347-359. https://doi.org/10.12989/anr.2021.11.4.347.
Tounsi, A., Al-Dulaijan, S.U., Al-Osta, M.A., Chikh, A., Al-Zahrani, M.M., Sharif, A. and Tounsi, A. (2020), "A four variable trigonometric integral plate theory for hygro-thermo-mechanical bending analysis of AFG ceramic-metal plates resting on a two-parameter elastic foundation", *Steel Compos. Struct.*, **34**(4), 511-524. https://doi.org/10.12989/scs.2020.34.4.511.
Tran, L.V., Ly, H.A., Lee, J., Wahab, M.A. and Nguyen-Xuan, H. (2015), "Vibration analysis of cracked FGM plates using higher-order shear deformation theory and extended isogeometric approach", *Int. J. Mech. Sci.*, **96-97**, 65-78. https://doi.org/10.1016/j.ijmecsci.2015.03.003.
Wattanasakulponga, N. and Ungbhakornb, V. (2014), "Linear and nonlinear vibration analysis of elastically restrained ends FGM beams with porosities", *Aerosp. Sci. Technol.*, **32**(1), 111-120. https://doi.org/10.1016/j.ast.2013.12.002.
Xiang, Y., Wang, C.M. and Kitipornchai, S. (1994), "Exact vibration solution for initially stressed Mindlin plates on Pasternak foundation", *Int. J. Mech. Sci*., **36**, 311-316. https://doi.org/10.1016/0020-7403(94)90037-X.
Zhang, D.G. and Zhou, H.M. (2015), "Mechanical and thermal post-buckling analysis of FGM plates with various supported boundaries resting on nonlinear elastic foundations", *Thin Wall. Struct.*, **89**, 142-151. https://doi.org/10.1016/j.tws.2014.12.021.
Zhang, D.G. and Zhou, Y.H. (2008), "A theoretical analysis of FGM thin plates based on physical neutral surface", *Comput. Mater. Sci.*, **44**(2), 716-720. https://doi.org/10.1016/j.commatsci.2008.05.016.
Zhou, D., Cheung, Y.K., Lo, S.H. and Au, F.T.K. (2004), "Three-dimensional vibration analysis of rectangular thick plates on Pasternak foundations", *Int. J. Numer. Meth. Eng*., **59**(10), 1313-1334. https://doi.org/10.1002/nme.915.
Zohra, A., Benferhat, R., Tahar, H.D. and Tounsi, A. (2021), "Analysis on the buckling of imperfect functionally graded sandwich plates using new modified power-law formulations", *Struct. Eng. Mech.*, **77**(6), 797-807. http://doi.org/10.12989/sem.2021.77.6.797.

CC